ChemistryOpen

Research Article
doi.org/10.1002/open.202200239

Chemistry Europe
European Chemical Societies Publishing

www.chemistryopen.org

Poly(vinyl alcohol)/*Premna Oblongifolia* Merr. Extract/Glutaraldehyde/Carbon Nanotube (VOGC)-Based Composite Hydrogel: A Potential Candidate for Controlled-Release Materials

Hendrawan Hendrawan,* Hafiz Aji Aziz, Nina Haryati, and Fitri Khoerunnisa[a]

A hydrogel based on poly(vinyl alcohol) (V), *Premna Oblongifolia* Merr. extract (O), glutaraldehyde (G), and carbon nanotubes (C) has been synthesized in search of candidates to develop controlled-release fertilizers (CRF). Referring to previous studies, O and C can be considered as two materials that have potential as modifiers in synthesizing CRF. This work is comprised of hydrogel synthesis, their characterisation, including measuring swelling ratio (*SR*) and water retention (*WR*) of VOG_m, VOG_e, VOG_mC_3, VOG_mC_5, VOG_mC_7, VOG_mC_7-KCl, and release behaviour of KCl from VOG_mC_7-KCl. We found that C interacts physically with VOG, increased the surface roughness of VOG_m, and reduced the VOG_m crystallite size. The addition of KCl into VOG_mC_7 reduced the pore size and increased the structural density of VOG_mC_7. The thickness and the C content of VOG affected its *SR* and *WR*. The addition of KCl into VOG_mC_7 reduced its SR, but did not significantly affect its WR.

Introduction

The availability of nutrients in sufficient quantities at the right time, in accordance with the plants' need, is a desirable farming condition to get good crop yields at low cost, and furthermore avoiding the risk of environmental damage. However, this condition is not easy to realise. In practice, the use of fertilizer is consequential to economy, crop yield, and environment, especially when the use of fertilizer is not controlled.[1–5] Conventional sprinkled fertilizer is relatively riskier in term of leaching and erosion by rainwater. For example, more than 50% of urea in demineralized water undergoes release at 24 °C in the first 30 s, and dissolves completely within 3–5 min.[6] Extremely fast release rates of fertilizer can lead to excessively high concentration of fertilizer in the vicinity of plants, which can cause unexpected side effects either in the target area or in the surrounding environment.[7] The content of nitrate and phosphate in fertilizer/nutrient released into surface water can cause eutrophication and/or explosion of algae population.[8,9] This can reduce the amount of sunlight that can penetrate into the bottom of the water and possibly compete with other aquatic fauna in term of oxygen consumption.[10]

Controlled-release fertilizer (CRF) has been considered as an alternative to control the rate of release of fertilizer or nutrient.[4,11–14] CRF have many advantages over conventional fertilizers. They are able to reduce the level of fertilizer loss from the soil, prolonging the availability of nutrient/fertilizer around the plant, increasing fertilizer efficiency, lowering the frequency of fertilizer use, minimizing negative impacts due to over-dose, and reducing toxicity.[14–16] It has also been proven that controlled-release NPK compound fertilizers have the ability to improve water retention of soil and fertilizer efficiency.[17]

One of the CRF agents that are commonly used is hydrogel, which is a three-dimensional polymer network that can retain large amounts of water but is relatively insoluble or retain impregnated material for a long enough period in water.[18,19] Structurally, the hydrogel network can be formed by cross-linking or by physical linkage.[20,21] This property is very advantageous because it provides researchers with opportunities to customize the material. Hydrogel can absorb and release water and nutrient proportionally when needed by plant. This property allows plants to always have supply of water and nutrient over a long period of time. Therefore, the hydrogel has the potential to be used as CRF material.

Poly(vinyl alcohol) can be considered as a material that has good properties as a precursor for synthesizing hydrogels because of its hydrophilicity and affinity to form gels. Poly(vinyl alcohol) gel is also considered as a useful biomaterial because of its low toxicity and high biocompatibility.[22] The physico-chemical properties and performance of material release agent resulted from crosslinking of poly(vinyl alcohol) with glutaraldehyde have been reported in some publications.[23–27] Meanwhile, the addition of *Premna oblongifolia* Merr. extract into the poly(vinyl alcohol)-glutaraldehyde mix was able to improve water uptaking performance, water retention, and reduce nutrient release to demineralized water media, but it reduces the hydrogel mechanical strength.[28] On the other hand, the application of carbon nanotube in the synthesis of composite polymers can improve their mechanical properties.[29] In addition, several researchers have found that the addition of

[a] *Dr. H. Hendrawan, H. A. Aziz, N. Haryati, Dr. F. Khoerunnisa*
Department of Chemistry
Universitas Pendidikan Indonesia
Jl, Dr. Setiabudhi No. 229 Bandung
40154. Jawa Barat (Indonesia)
E-mail: hendrawan@upi.edu

carbon nanotubes at the optimum composition into the hydrogel can increase the swelling of the hydrogel, eventually improving the performance of the hydrogel as CRF materials.[30,31] Carbon nanotubes are a carbon structure that is shaped like a cylinder with a diameter in the nanometer scale. Since the discovery of the carbon nanotube structure, many properties of carbon nanotubes have been studied such as their unique mechanical, electrical, and thermal properties, as well as the strong interaction with the polymer matrix resulting from the nanoscale structure and the very large interfacial area of carbon nanotubes.[32,33] In this research, the performance of CRF hydrogel based on poly(vinyl alcohol), *Premna oblongifolia* Merr. extract, and carbon nanotube was studied with glutaraldehyde as crosslinker, and potassium chloride as nutrient.

Results and Discussion

Physicochemical Characteristics

To simplify the notation for synthesized hydrogels, we denote the hydrogels using abbreviations of components, as well as measurement of the hydrogels. Poly(vinyl alcohol), *Premna oblongifolia* Merr. extract, glutaraldehyde, and carbon nanotubes solution are denoted as V, O, G, and C respectively. Because the main matrix of the hydrogel is just the hydrogels, namely poly(vinyl alcohol), *Premna oblongifolia* Merr. extract, and glutaraldehyde, all hydrogel will have VOG as the main matrix, with the thickness of the matrix denoted as m (French, *mince*) for thin hydrogel, and e (French, *épais*) for thick hydrogel. For hydrogel with carbon nanotubes dispersed inside the matrix, it was denoted with the addition of C_x, with x is the volume (mL) of the carbon nanotube solution added into the mixture of the hydrogel. Therefore, thin hydrogel with 7 mL of carbon nanotube solutions added will be denoted as VOG_mC_7. For hydrogel that was immersed in KCl solution, we append '-KCl' into the hydrogel notation.

FTIR characterization. The structures of VOG_m, VOG_mC_7, and VOG_mC_7-KCl hydrogels, as represented by FTIR spectra of their functional groups, are presented in Figure 1.

As shown in Figure 1, VOG_m, VOG_mC_7, and VOG_mC_7-KCl hydrogels have similar features in their FTIR spectra. In the three hydrogels, the presence of peaks at the wave number of 3400 cm^{-1} indicate the presence of O–H functional groups; peaks at around the wave number of 2800–2900 cm^{-1} indicate the presence of C–H sp^3, those at the wave number of 1700 cm^{-1} indicate an absorption of C=O, and the absorption at the wave number of 1000–1300 cm^{-1} indicates the presence of the C–O/C–O–C functional group.

The addition of carbon nanotube into VOG_m (VOG_mC_7 hydrogel), in general, produced a significant increase in absorption. However, despite the observed increase in intensity, there is no loss or gain of peaks, indicating that the interaction between VOG_m hydrogel matrix and carbon nanotube may occur only physically, and not chemically. The increasing absorption intensity at the wave numbers of 3400 cm^{-1}, 1700 cm^{-1}, and 1000–1300 cm^{-1} indicates the presence of O–H, C=O, and C–O/C–O–C groups originating from functionalized carbon nanotubes.[33] Meanwhile, the increase in absorption at wave numbers of 2800–2900 cm^{-1} (absorption peak of CH sp^3) is probably due to the strong interaction between the functional group of CH sp^3 and the functional group from carbon nanotubes.

Impregnation of KCl into VOG_mC_7 (VOG_mC_7-KCl hydrogel), however, reduced the absorption intensity. The impregnated potassium chloride within the VOG_mC_7 hydrogel matrix interfered with the ability of functional groups to vibrate in the hydrogel matrix. In terms of contour, the addition of KCl causes the peak of VOG_mC_7-KCl to broaden. A significant decrease in the absorption intensity in the vibrational region of the hydroxyl group after KCl impregnation into the composite hydrogel indicated that the addition of KCl can reduce water affinity of the hydrogel which would induce a reduction in the swelling ratio.[36]

SEM Characterization. The surface morphology of VOG_m, VOG_mC_7 and VOG_mC_7-KCl hydrogels were imaged by SEM instrumentation as presented as in Figure 2.

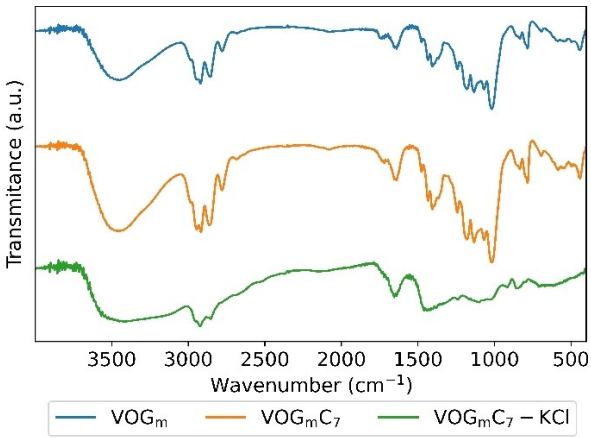

Figure 1. FTIR Spectra of VOG_m, VOG_mC_7, VOG_mC_7-KCl.

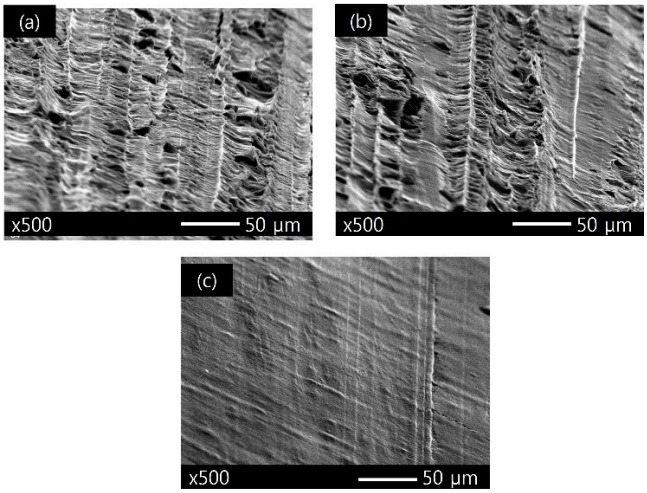

Figure 2. SEM image of (a) VOG_m, (b) VOG_mC_7, and (c) VOG_mC_7-KCl.

Figures 2(a) and 2(b) show that the pores on the surface of VOG_mC_7 hydrogel are more homogeneous than that on the surface of the VOG_m hydrogel. This fact will be corroborated in the next section, on the swelling ratio. This suggested that carbon nanotubes can increase the porosity of the hydrogel; by dispersing themselves in the matrix and the surface of hydrogel so as to affect the hydrogel matrix by interacting with the hydrogel functional groups.

In stark contrast with the surface morphology of the VOG_m and VOG_mC_7 hydrogels, the surface morphology of the VOG_mC_7-KCl hydrogel appeared to be very smooth, indicating that the pores of VOG_mC_7-KCl are either very small or almost closed (Figure 2(c)). This may be because the impregnated KCl entered and filled the pores of the VOG_mC_7-KCl hydrogel, thus causing the VOG_mC_7-KCl hydrogel to be physically more rigid. It is also worth to note that KCl, in the form of its cation and anion, could also act like a natural crosslinkers thereby increasing the structure density of the hydrogel. Polymer materials with higher crosslinker degree will also have a more compact network structure, which might reduce the swelling ability of the hydrogel.[37]

XRD Characterization. The X-ray diffractograms of VOG_m, VOG_mC_7, and VOG_mC_7-KCl are presented in Figure 3, and their parameters related to the Scherrer and Bragg equations[38] are represented in Table 1.

As can be seen in Figure 3 regarding the diffractograms of VOG_m and VOG_mC_7, there are wide peaks at $2\theta = 18.67°$ (VOG_m) and $2\theta = 18.17°$ (VOG_mC_7). This indicates that the VOG_m and the VOG_mC_7 hydrogels are predominantly in the form of amorphous structure. Other than inducing small shift to the left in the diffractogram, we also observe that the presence of carbon nanotubes in the matrix of VOG_mC_7 broadens the peak. Accordingly, as shown in Table 1, there is an increase in interlayer distance (d) from 0.475 nm in VOG_m to 0.488 nm in the VOG_mC_7 hydrogel, as well as a decrease in the mean crystallite size (L) from 1.305 nm to 1.196 nm. Interestingly, the impregnation of KCl into the matrix of VOG_mC_7 reduced the peak width, resulting in the value of interlayer distance of 0.461 nm for VOG_mC_7-KCl with mean crystallite size of 2.053 nm. This confirms that the impregnation of KCl into the matrix of the composite hydrogel would produce a more structured material.

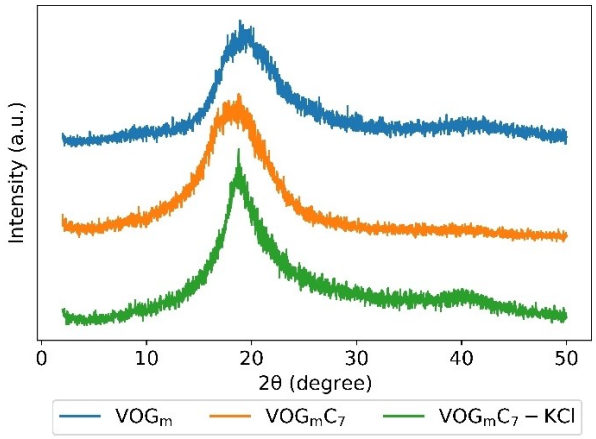

Figure 3. X-ray diffractogram of VOG, VOG_mC_7, and VOG_mC_7-KCl using X-ray source Cu Kα (λ = 0.154 nm).

Table 1. Parameters deducted from X-ray diffractograms of VOG, VOG_mC_7, and VOG_mC_7-KCl [after normalizing; with values of λ = 0.154 nm (Cu Kα X-ray source), n = 1, and K = 0.92]

Sample	2θ [°]	d [nm]	β [rad]	L [nm]
VOG_m	18.67	0.475	0.11	1.305
VOG_mC_7	18.17	0.488	0.12	1.196
VOG_mC_7-KCl	19.25	0.461	0.07	2.053

Performance Characteristics

Performance of VOG hydrogels. In this work, the description of VOG hydrogel performance is represented using the swelling ratio and water retention parameters. The measurements of these two performance parameters were carried out for the VOG_m (thickness 0.038 mm) and VOG_e (thickness 3.000 mm) hydrogels.

Swelling Ratio. The weighing of the mass of hydrogel was carried out both for the VOG hydrogel before immersion (as time $t = 0$ h) and that after soaking, which was carried out when the immersion time had reached 24 h, 48 h, 72 h, 144 h, 168 h, 192 h, 216 h, 240 h, 312 h, and 336 h. The swelling ratio profiles of VOG_m and VOG_e are given in Figure 4.

The graph in Figure 4 shows that the thickness of the VOG hydrogel flake produced two different swelling ratio profiles. The swelling ratio of VOG_m is much greater than that of VOG_e. This fact indicates that the thickness of hydrogels influences their ability to accommodate water. The thin sheet of hydrogel has a wider specific surface exposure to water which allows water to enter the hydrogel quickly. In addition, the rigidity of the thick-sheet hydrogel reduces the hydrogel capacity to accommodate water.

Water Retention. Water retention profiles of VOG_m and VOG_e, and the soil as a blank standard, are shown in Figure 5.

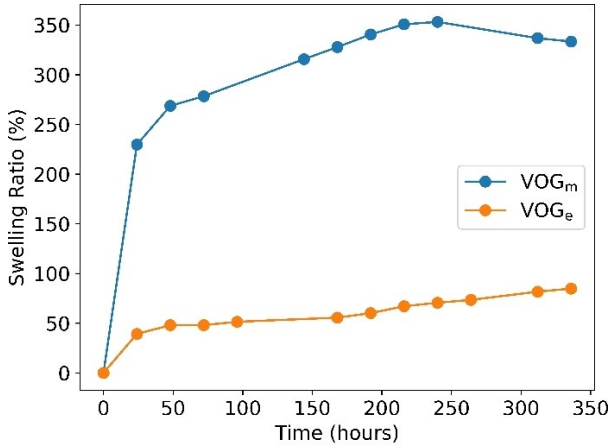

Figure 4. Swelling ratios of VOG_m (0.038 mm) and VOG_e (3.000 mm).

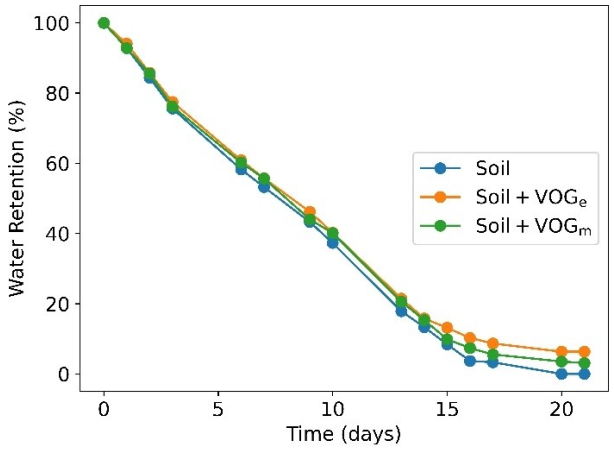

Figure 5. Water retention of VOG$_m$ and VOG$_e$.

The graph in Figure 5 shows that the water retention of soil to which VOG$_m$ had been added was superior compared to both soil with VOG$_e$ and soil without hydrogel (blank). This fact is in line with the hydrogels swelling ratio profile. In addition to its better ability to accommodate water, which is indicated by its swelling ratio, VOG$_m$ also has a relatively strong interaction with water, as shown by its water retention.

Performance of VOG$_m$C$_x$ hydrogels. VOG$_m$C$_x$ hydrogel performance is measured by the swelling ratio and water retention parameters. The measurement of these two performance parameters were carried out for VOG$_m$C$_3$, VOG$_m$C$_5$, and VOG$_m$C$_7$.

Swelling Ratio. VOG$_m$C$_x$ hydrogels are the hydrogels formed from VOG$_m$ hydrogel with carbon nanotubes added during their preparation. To see the effect of addition of carbon nanotubes to the VOG hydrogel matrices, various amounts of carbon nanotubes were added into the mix of VOG$_m$ hydrogels. The addition of carbon nanotubes into the mix of VOG$_m$ was varied from 3 mL, 5 mL, up to 7 mL, which respectively produced VOG$_m$C$_3$, VOG$_m$C$_5$, and VOG$_m$C$_7$ hydrogels. The swelling ratio profiles of VOG$_m$C$_x$ hydrogels are given in Figure 6.

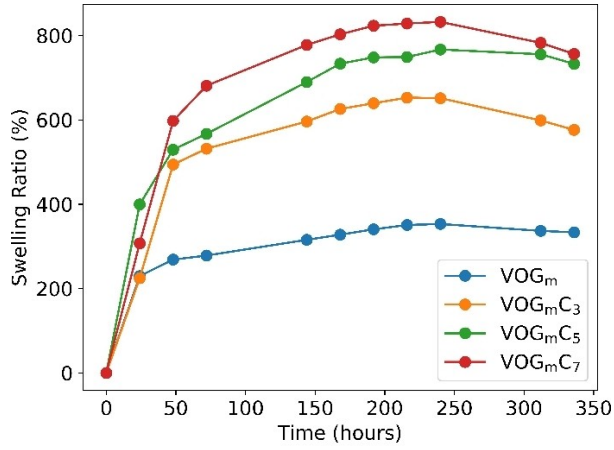

Figure 6. Swelling ratio profiles VOG$_m$, i.e. VOG$_m$C$_3$, VOG$_m$C$_5$, andVOG$_m$C$_7$.

The graph in Figure 6 shows that for the addition of carbon nanotubes into the VOG$_m$ hydrogel matrix, the swelling ratio tends to increase as the amount of carbon nanotube in the matrix increases. Referring to the results of SEM instrumentation, as shown in Figure 2, the addition of carbon nanotubes into the VOG$_m$ hydrogel matrix effectively increases the pores on the surface, which consequently increases the water flux into the inner part of the hydrogel. A study conducted by Vural et al.[39] concerning the effect of carbon nanotube content on the cross-link density, viscoelasticity, and swelling behaviour of polyethylene glycol monoacrylate (PEGMA), showed that increasing the concentration of carbon nanotubes added to the hydrogel matrix resulted in a decrease in the cross-link density of the hydrogel. Additionally, the addition of carbon nanotubes into hydrogels has been reported to increase the swelling ability of the hydrogel, thus increasing the performance of the hydrogel as a CRF material.[30,31] In the framework of these statements, the addition of carbon nanotubes into the VOG$_m$ hydrogel material reduces the cross-link density, increases the ability to accommodate water, which increases with the quantity of added carbon nanotubes. The graph in Figure 6 shows that the swelling profile of the VOG$_m$C$_x$ hydrogel increased with the increase in the amount of carbon nanotube volume added (increasing x value). The highest swelling ratio value was achieved when the volume of CNT added was 7 mL, which was 832.4 %. This finding confirms that the more carbon nanotubes are added, the lower the cross-link density.

As shown in Figure 6, the maximum values of the swelling ratio for VOG$_m$, VOG$_m$C$_3$, VOG$_m$C$_5$, and VOG$_m$C$_7$ were observed at the 240th hour of immersion. In that time, there is a regular increase in swelling ratio starting from VOG$_m$ up to VOG$_m$C$_7$. However, the gap in swelling ratio of two adjacent hydrogels decreased as the added volume of carbon nanotube increased. The gap of swelling ratio between VOG$_m$C$_5$ and VOG$_m$C$_7$ is smaller than that between VOG$_m$C$_3$ and VOG$_m$C$_5$, and much smaller compared to that between VOG$_m$ and VOG$_m$C$_3$. Based on that fact, we thus deduced that any addition of CNT for further higher value of x into the VOG$_m$ matrix will not produce significant increase in swelling ratio. Therefore, we stopped the optimization at VOG$_m$C$_7$.

Water Retention. Water retention profiles of the VOG$_m$C$_x$ hydrogels are given in Figure 7; Figure 7(a) shows the profiles during the normal period and 7(b) during the period of the 14th–29th day.

It can be seen in Figure 7(a) that the water content in all media, which are soil without hydrogel, soil with VOG$_m$, and soil with VOG$_m$C$_x$, decreased drastically with similar rates until approximately the 14th day; afterwards, the water mass decreased at different rate during the later period. In this later period (time segment 14th up to the 29th day), as shown in Figure 7(b), it appears that the medium with hydrogel were able to retain water better than the soil media. The presence of carbon nanotubes in the hydrogel matrices also increases the ability of the media to retain water, albeit not significantly in comparison to VOG$_m$. Likewise, for the quantity of carbon nanotubes added, the more carbon nanotube added, the higher the ability of media to retain water. In this case, the water

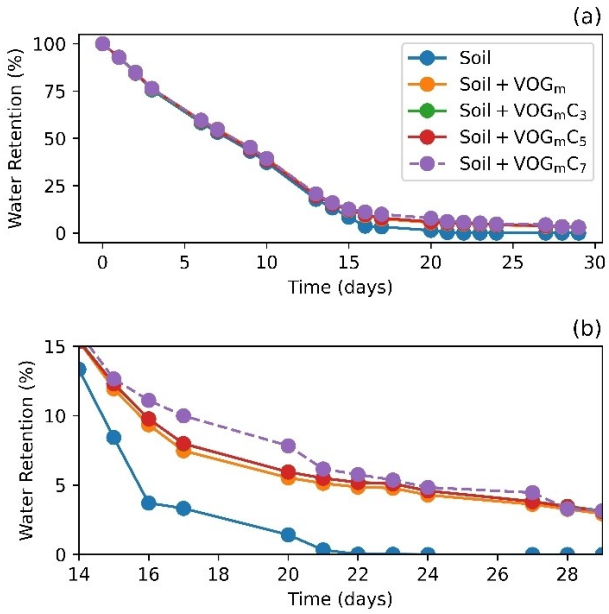

Figure 7. Water retention of VOG_m, i.e., VOG_mC_3, VOG_mC_5, VOG_mC_7; (a) during the normal period, (b) during the period of the 14^{th}–29^{th} day.

retention of the VOG_mC_7 hydrogel is slightly higher than that of the other VOG_mC_x hydrogel within the later period of measurement.

Referring to the procedure of the water retention experiment, there must be at least two factors that should be considered that can affect the water retention profile, namely water absorption by media and evaporation from the system. As the water had been added into the media, both soil and hydrogel absorbed water; then, after a while, the process of evaporation begun. As the quantity of soil is much higher than that of the hydrogel, most of the added water was absorbed by soil, so that at the early period of treatment, the mass loss would be dominated by the water evaporation from the soil. This caused the rate of water evaporation for all media up to the 14^{th} day to be very similar to each other (Figure 7(a)), which implies that any process involving the hydrogels did not significantly affect the mass loss from the system. As the water content of soil diminished, the mass loss then became predominantly governed by processes involving the hydrogels. Without the presence of hydrogel, the mass of the system will decrease rapidly. This is also the reason why the hydrogel-free soil during, the later period, loses all of its water. In contrast, soil with added hydrogel can retain water for longer periods of time. Within those hydrogel-containing systems, there is variation with respect to their water retention profiles, where the system with the VOG_mC_7 hydrogel tends to retain water better than the others. The difference in their water-retaining ability is possibly due to the difference in hydrogel ability to resist water percolation and evaporation. In accordance with Figure 6, VOG_mC_7 exhibits the highest swelling ratio indicating its ability to accommodate more water. This indicates that VOG_mC_7 has a more flexible structure that can adapt to changes in its physical surroundings. This characteristic, which is possibly due to its voids and microcrack profile, will produce a more robust physical state, better able to resist fracture propagation, and eventually produce a better ability to resist water evaporation.

Performance of VOG_mC_7-KCl. The performance of VOG_mC_7-KCl was characterised by three parameters, namely swelling ratio, water retention, and release behaviour.

Swelling Ratio. The swelling ratio profiles of VOG_m, VOG_mC_7, and VOG_mC_7-KCl hydrogels are presented in Figure 8.

As can be seen in Figure 8, the swelling ability of VOG_mC_7 is significantly higher than that of VOG_m. However due to the presence of KCl, it was reduced back to a bit higher level than that of VOG_m. As a quantitative comparison, the maximum swelling ratio of VOG_m was 553.1%, that of VOG_mC_7 was 832.3%, and that of VOG_mC_7-KCl was 430.7%. The difference in performance between VOG_m and VOG_mC_7 could be attributed to the dispersed carbon nanotubes in the VOG_m matrix and the nature of the VOG_m itself as indicated by the result of FTIR, SEM, and XRD measurements. The dispersion of carbon nanotubes in the VOG_m hydrogel matrix reduced the cross-link density, causing the structure of VOG_mC_7 to be significantly more porous, which is in agreement with the finding of Vural et al.[39] Compared to VOG_m, the features of the swelling ratio of VOG_mC_7 indicate that the VOG_mC_7 has a structure that allows the gel to imbibe more water. The FTIR spectra for the two gels did not show any significant differences (Figure 1), indicating that the carbon nanotubes are only dispersed in between the framework of VOG_m. This is further supported the SEM result, as shown in Figure 2(b), which indicates that VOG_mC_7 is more porous than VOG_m. Additionally, the XRD diffractograms (Figure 3 and Table 1) show that the interlayer distance value (*d*) of VOG_m is smaller than that of VOG_mC_7, while the crystallite size of VOG_m is bigger than that of VOG_mC_7. This increase in interlayer distance of VOG_mC_7 also supports the argument for its high swelling ability.

As shown in Figure 2(c), the surface morphology of VOG_mC_7-KCl has very small pores, which means that the presence of KCl reduced the hydrogel pore size. This phenomenon makes it more difficult for water to enter the hydrogel matrix. Although

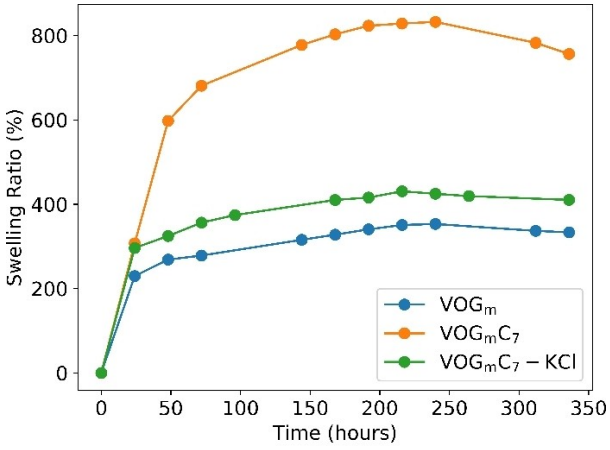

Figure 8. Swelling ratios of VOG_m, VOG_mC_7, and VOG_mC_7-KCl.

the rate of swelling of the hydrogels is not significantly different, the water accommodation capacity of VOG_mC_7-KCl is much lower than that of VOG_mC_7 (Figure 8). This indicates that there was a structural change in the interior of the hydrogel caused by the presence of KCl. This is supported by the evidence that the value of the interlayer distance of VOG_mC_7-KCl is smaller than that of VOG_mC_7 (Table 1). The presence of potassium ions in the gel can increase the material density. In VOG_mC_7-KCl, there should be interaction between the potassium ions and the carboxyl and hydroxyl groups present in the VOG_mC_7 hydrogel, which results in the decrease in the hydrophilicity of the VOG_mC_7-KCl hydrogel, and consequently a decrease in its swelling performance.[36] The fact that the water accommodation capacity of VOG_mC_7-KCl is higher than that of VOG_m can be explained by the argument that the potassium ions inside the gel may attract more water.

Figure 8 also shows that there is a decrease in swelling ratio of the VOG_mC_7 hydrogel starting at the 240th hour and lasting at least up to the 340th hour of the recorded data. Meanwhile, the curves for VOG_m and VOG_mC_7-KCl both remained stable until the end of the measurement. These phenomena could be explained through the concept of fracture dynamics.[40] The VOG_mC_7 hydrogel framework seems to have some micro-cracks. As the VOG_mC_7 hydrogel swells due to water absorption, the microcracks grew to a point such that the gel reached the fracture condition at around the 240th hour, which can be considered a delayed fracture.[41] Meanwhile, the addition of KCl into the hydrogel matrix was able to strengthen the hydrogel structure, which was able to avoid crack elongation so as to delay fracture within the measurement period. Likewise, the swelling ratio-to-time curve profile for VOG_m is similar to the swelling ratio-to-time curve for VOG_mC_7-KCl. The VOG_m has a strong gel framework due to the cross-linking between its components. In this context, the water impingement on the VOG_m hydrogel matrix is not strong enough to increase the length of the micro-cracks in the hydrogel. In other words, the addition of carbon nanotubes reduces the strength of the VOG_m hydrogel framework, but the addition of KCl to the VOG_mC_7 hydrogel matrix is able to restore the hydrogel strength to a similar level compared to the VOG_m hydrogel.

In comparison with a previous study, which used *Gracilaria* as the source of natural polymer to form a Gracilaria/Poly(vinyl alcohol)/Glutaraldehyde/Carbon nanotube hydrogel (GR/PVA/GA/CNT), [23] VOG_mC_7 has a higher swelling ratio. The maximum swelling ratio of VOG_mC_7 is 832.38 % with an immersion time of 10 days, while the maximum swelling ratio of GR/PVA/GA/CNT is just 182.43 % with an immersion time of 9 days. This suggests that VOG_mC_7 is more expandable than GR/PVA/GA/CNT, and thus can accommodate as much as 4 times more water in its matrix.

Water Retention. The performance of VOG_m, VOG_mC_7, and VOG_mC_7-KCl in term of water retention is presented in Figure 9(a), and for the sake of clarity, the data for the later period of the treatment is presented in Figure 9(b).

Figure 9(a) shows that the water content in all media (soil without hydrogel, soil with VOG_m hydrogel, soil with VOG_mC_7 hydrogel, soil with VOG_mC_7-KCl hydrogel) decreased drastically

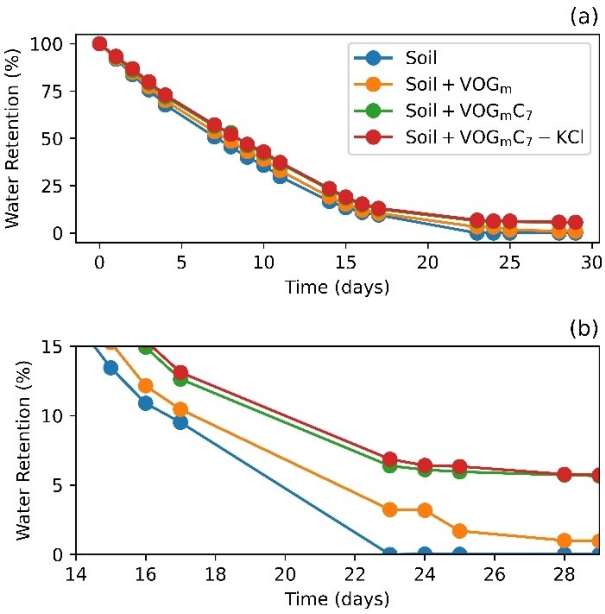

Figure 9. Water retention of VOG_m, VOG_mC_7, and VOG_mC_7-KCl; (a) during the normal period, (b) during the period of the 14th – 29th day

with relatively the same rate until approximately the 14th da after which the decrease in the mass of water in the media is slightly different for each medium during the rest of the measurement period. In the later period of treatment, namely at the time segment of the 14th up to the 29th day, as shown in Figure 9(b), it seems that the media with hydrogel were able to retain water better compared to the soil without hydrogel.

The presence of carbon nanotubes in the hydrogel matrices also increases the ability of the media to retain water. The more carbon nanotubes are added, the higher the ability of media to retain water. Although the presence of nutrient (KCl) was able to reduce the swelling ability of VOG_mC_7 hydrogel (Figure 9(a)), it did not significantly affect the water retention (Figure 9(b)).

In most cases, there is usually a correlation between swelling ratio and water retention. However, despite the similarity between VOG_mC_7-KCl swelling ratio profile with VOG_m, its water retention profile is more in line with that of VOG_mC_7.

The water retention profile of the hydrogels as presented in Figures 9(a) and 9(b), in principle, can be explained by the same argument used to explain the water retention profile of the VOG_mC_x hydrogels (Figures 7(a) and 7(b)). Additionally, the higher water retention ability of VOG_mC_7-KCl in comparison to that of VOG_mC_7 can be explained by the contribution due to entrapped potassium ion hydration, which then increases the hydrogel's ability to resist water evaporation.

Release Behaviour of VOG_mC_7-KCl. The KCl release behaviour profile of the VOG_mC_7 hydrogel is shown as the mass of KCl released from the hydrogel into demineralized water media, as shown in Figure 10. It should be emphasized that the impregnation of KCl into the gel was done by immersing the hydrogel into KCl solution. We used a 1.0 M solution of KCl for two reasons. Firstly, potassium is one of macronutrient for plant so that the high concentration of KCl may give us some

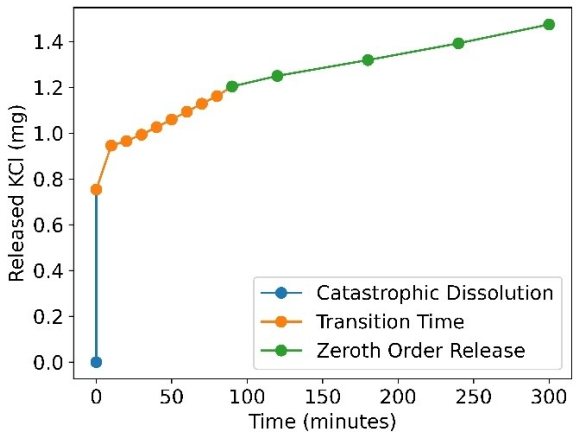

Figure 10. Mass of released potassium chloride from VOG_mC_7-KCl into demineralized water.

information about the impregnation capacity of the gel. Secondly, it is to ensure that the KCl remains present in the hydrogel during the study of release kinetics of KCl from the hydrogel.

The graph in Figure 10 shows that, in general, the release of KCl from the hydrogel into water media was very fast in the initial phase of immersion (about the first 5 s), then the release rate slowed down up to the 90th minute, and then reached a steady slow release until the end of the measurement period. We propose that the release behaviour can be divided into three distinct phases, which are catastrophic dissolution (0 to 5 s), transition time (5 s to 90 min), and zeroth order release (90 to 300 min). A possible mechanism for this process is visualized in Figure 11.

As illustrated in Figure 11, at the initial period, the release seems to occur catastrophically, and for convenience we thus called it catastrophic dissolution. During this phase, 0.75357 mg of KCl or 3.841 % of the total KCl contained in the hydrogel before immersion (19.61908 mg) was dissolved into water media within 5 s or less. This phenomenon indicates that the dissolved KCl is that settled at the outside of the hydrogel and is not directly attached to the hydrogel in any way.

In the second phase (5 s up to 90 min), the dissolution rate slowed down, indicated by the decrease in the steepness of the curve. The release behaviour in this phase is possibly governed by both the presence of the KCl on the surface and the KCl inside the hydrogel. The KCl present in the inner part of hydrogel has begun to be released into the medium. Compared to the KCl that has already been dissolved at the first phase of immersion, the rest of KCl around the outer surface is sticking

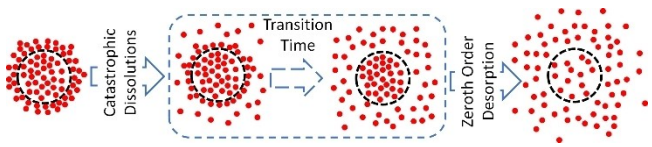

Figure 11. Illustration of releasing KCl from VOG_mC_7-KCl into demineralized water.

to the surface of the hydrogel, generating a more structured layer at the surface, inhibiting ion leaching from the inner part, and eventually slowing down the release. Followingly, the KCl that remains at the surface of the hydrogel gradually dissolved into the medium as the water shear worked on it. At the same time, water has gradually penetrated the surface of hydrogel, hydrating the KCl located in the inner part of hydrogel, driving the KCl to the surface, thus replacing the previously dissolved surface ion before it itself eventually dissolved into the bulk water. At the beginning of this process, the release is still dominated by the contribution of the KCl from the outermost part. As time goes by, this process becomes gradually dominated by release of KCl from the inner part of the hydrogel.

At the 90 min mark, the cleansing of KCl from the surface of the hydrogel should have been completed and the total released KCl has reached 1.2038 mg or 6.13 %. Starting from this point, the released KCl should be considered as originating purely from inner part of the hydrogel. This means that the mass of KCl that remains in the hydrogel is 18.4152 mg. The calculation of the desorption kinetics of KCl into water starts from the 90th minute of immersion so that the initial condition of the system that we use is when the KCl contained in hydrogel is 18.4152 mg, and the KCl dissolved in water is 1.2038 mg. The plot of the mass of KCl released against time (period of 90 to 300 min) follows zeroth-order kinetics with the rate Equation (1)

$$m_t = m_0 + kt \quad (1)$$

where m_t and m_o are the mass of KCl at time t (calculated starting after the first 90 min) and time $t=0$ when the experiment has been running for 90 min, while k is the rate constant with value of 1.2645×10^{-3} mg/s. In the framework of controlled-release fertilizer (CRF) development, the release profile following zeroth order is very beneficial because the quantity of nutrients in the media will be more controllable.

There are several factors that might play a role in affecting this process, including hydration, dissolution, surface forces, and diffusion. The overall release mechanism may involve the dissolution of outer layer of KCl around the surface, dissolution of the KCl stuck to the hydrogel surface, intrusion of water into the hydrogel, hydration of KCl inside the gel, diffusion of hydrated KCl from the hydrogel onto the surface, and their dissolution into the bulk, where the release at transition phase is a mixed contribution from surface cleansing and desorption.

The fact that VOG_mC_7 has higher swelling ratio in comparison to VOG_m (Figure 8), high water retention (Figure 9), and is characterized by zeroth order release kinetics indicates that VOG_mC_7 has good water capacity, long-lasting water retention, and releases the nutrient only depending on its own characteristics. Therefore, VOG_mC_7 may be considered as a promising material that can be developed for CRF.

Conclusion

The interaction between carbon nanotubes and the VOG_m matrix may possibly occur only physically. The surface of VOG_mC_7 is rougher than that of VOG_m, meanwhile the addition of KCl to the VOG_mC_7 hydrogel matrix reduces or masks the pores that are present on the surface of the hydrogel. The presence of carbon nanotubes in the VOG_m matrix reduces its structural compactness, while the addition of KCl into the matrix of VOG_mC_7 induces the formation of a denser and more structured material. A VOG_m hydrogel flake has higher swelling and water retention ability than VOG_e. The VOG_mC_x hydrogel with higher carbon nanotube content has greater swelling and water retention ability. The impregnation of KCl into the VOG_mC_7 hydrogel matrix reduced the swelling ability of VOG_mC_7 dramatically. However, the water retention ability of VOG_mC_7-KCl hydrogel is stronger than that of VOG_mC_7, and VOG_m. The release of KCl from VOG_mC_7-KCl was started by a catastrophic dissolution of KCl from the surface of the hydrogel, followed by surface cleansing and desorption during a transition period, and ended with the desorption of KCl from inside the hydrogel following zeroth-order desorption kinetics with a rate constant of 1.2645×10^{-3} mg/s. The VOG_mC_7 hydrogel has been shown to have a good swelling and water retention capability, as well as being able to reduce the KCl release rate, therefore it is reasonable to be further developed as a candidate for controlled-release materials.

Experimental Section

Materials and Instruments

The materials used in this study were *Premna oblongifolia* Merr. extract (local), poly(vinyl alcohol) (Brataco, Singapore), glutaraldehyde (p.a.) (Merck, Germany), methanol (p.a.) (Merck, Germany), sulfuric acid (Merck, Germany), acetic acid (p.a.) (Merck, Germany), graphene oxide, functionalised multiwall carbon nanotubes, KCl, soil and demineralized water.

The main instrument used were FTIR spectroscopy, Shimadzu (Japan), Scanning Electron Spectroscopy (SEM) JEOL JSM-6510LA (Japan), flame photometer corning 410 made in CIBA-Corning, Madrid (Spain), X-ray Diffraction (XRD) Mini Flex600 made in Rigaku, Tokyo (Japan).

Preparation of Reactants

The solution of poly(vinyl alcohol) was prepared by dissolving 10 mg of poly(vinyl alcohol) powder in 50 mL of deionized water, and stirred while heated at 90 °C for about 3 h. The crosslinker solution was prepared by mixing methanol 50 %, acetic acid 10 %, sulfuric acid 10 %, and glutaraldehyde 1.25 % with a volume ratio 3:2:1:1, respectively. The dispersion of CNT was prepared by dissolving 1 mg of CNT into 100 mL of graphene oxide solution (1 % w/v in deionized water), then the solution was sonicated for about 30 min. POM extract was prepared by extracting 1000 mg of dry-powdered *Premna Oblongifolia* Merr. (100 mesh) in 100 mL of sodium hydroxide solution pH 10, stirred for about 1 h, after which the extract was separated from the residue.[42]

Preparation of Hydrogel

To simplify the notation for synthesized hydrogels, we denote the hydrogels using abbreviations of components, as well as measurement of the hydrogels. Poly(vinyl alcohol), *Premna oblongifolia* Merr. extract, glutaraldehyde, and carbon nanotubes solution are denoted as V, O, G, and C respectively. Because the main matrix of the hydrogel is just the hydrogels, Poly(vinyl alcohol), *Premna oblongifolia* Merr. extract, and glutaraldehyde, all hydrogel will have VOG as the main matrix, with the thickness of the matrix denoted as m (French, *mince*) for thin hydrogel, and e (French, *épais*) for thick hydrogel. For hydrogel with carbon nanotubes dispersed inside the matrix, it was denoted with the addition of C_x, with x is the volume (mL) of the carbon nanotube solution added into the mixture of the hydrogel. Therefore, thin hydrogel with 7 mL of carbon nanotube solutions added will be denoted as VOG_mC_7. For hydrogel that was immersed in KCl solution, we append '-KCl' into the hydrogel notation.

The prepared CRF hydrogels were (1) poly(vinyl alcohol) - *Premna oblongifolia* Merr. extract - glutaraldehyde hydrogels (VOG_y: VOG_m and VOG_e hydrogels); (2) poly(vinyl alcohol) - *Premna oblongifolia* Merr. extract - glutaraldehyde - carbon nanotube hydrogel (VOG_yC_x: VOG_mC_3, VOG_mC_5, and VOG_mC_7 hydrogels); and (3) KCl-impregnated VOG_mC_7 hydrogel (VOG_mC_7-KCl hydrogel).

The VOG_y and VOG_yC_x hydrogels were prepared by mixing their constituent components with composition as shown in Table 2, at 50 °C, while stirred for 7 min. The mixture was then poured into moulds, and dried at room temperature for 14 days for the thick flake . and 5 days for the thin flake .

The VOG_mC_7-KCl was prepared by immersing dried VOG_mC_7 hydrogel into 50 mL of 1.0 M KCl solution for 48 h, while gently stirring using a magnetic stirrer. The immersed hydrogel was then dried at room temperature for 30 min.

Physicochemical Characterization

The morphologies of the surface of hydrogels and KCl-impregnated hydrogel were analysed using scanning electron microscopy (SEM) model JEOL JSM-6510LA (Japan). The structure of the hydrogel, which is manifested in the functional group parameter, was analysed using FTIR spectroscopy, Shimadzu (Japan). The patterns of X-ray diffraction of hydrogel and KCl-impregnated hydrogel were measured at room temperature using X-ray Diffraction (XRD) Mini Flex600 made in Rigaku, Tokyo (Japan) using a CuKα X-ray source ($\lambda = 0.154$ nm).

Table 2. The matrix of volume of poly(vinyl alcohol), *Premna oblongifolia* Merr. extract, glutaraldehyde, and carbon nanotube used in preparation of the hydrogels

V [mL]	O [mL]	G [mL]	C [mL]	Name/ Symbol[a]
10	10	18	0	VOG_m
10	10	18	0	VOG_e
10	10	18	3	VOG_mC_3
10	10	18	5	VOG_mC_5
10	10	18	7	VOG_mC_7
10	10	18	7	VOG_mC_7-KCl

[a] m is the symbol for thin flake ; e is the symbol for thick flake ; V is the symbol for poly(vinyl alcohol); O is the symbol for *Premna oblongifolia* Merr. Extract; G is the symbol for glutaraldehyde; C is the symbol for carbon nanotube

Determination of Swelling Ratio

The swelling ratio test was carried out using gravimetric method. Six sets of dried synthesized hydrogel samples, namely VOG_m, VOG_e, VOG_mC_3, VOG_mC_5, VOG_mC_7, and VOG_mC_7-KCl, were weighed (W_d). Then, each sample was immersed in 25 mL of distilled water using a 100 mL beaker glass (7 pieces for each set of samples). This means that for six sets of hydrogels there must be 42 pieces of beaker glass. In every set of hydrogels, the hydrogel in the first container was removed after 24 h of immersion, dried for 30 min, then re-weighed. The mass of the hydrogel after immersion is denoted by W_s. The same treatment was carried out for all the other hydrogels after soaking for the specified time, namely 48 h, 72 h, 144 h, 168 h, 192 h, 216 h, 240 h, 312 h, and 336 h. Furthermore, the value of the Swelling Ratio (*SR*) of the hydrogel was calculated using the following Equation (2).[34,35]

$$\%SR = \frac{W_s - W_d}{W_d} \times 100 \quad (2)$$

Determination of Water Retention

A set of test protocol was made for each system water retention test. In this work, there were two protocols, namely a system without hydrogel and a system with hydrogel. The test system without hydrogel was 40 g of dry soil media, which was placed in a beaker glass. The hydrogel test system was made by adding a certain mass of dried VOG_m and VOG_e hydrogels into 40 g of dry soil that had been stored in a beaker glass. The dry mass was then referred to as the dry mass of the system (*W*). To each system, 25 mL of water was added, then weighed, and the mass was recorded as the initial wet mass (W_0). The three systems that already contain water were stored at room temperature, their masses were weighed every day at the same time, recorded as wet mass at a certain time, namely W_t. This work was carried out until the mass of the system remains relatively unchanged. The water retention value (%WR) of the systems were then calculated using the following relationship [Eq. (3)].[19]

$$\%WR = \frac{W_t - W}{W_0 - W} \times 100 \quad (3)$$

Determination of Release Behavior

Four pieces VOG_mC_7 with a dimension of $10 \times 10 \times 0.0038$ mm^3 were immersed in 50 mL of 1.0 M KCl solution for 48 h, while stirred gently using a magnetic stirrer, lifted using a piece of small porous spatula, then dried at room temperature for 30 min (hereinafter referred to as VOG_mC_7-KCl hydrogel). The remaining content of KCl in the solution used to load VOG_mC_7 was measured using a flame photometer corning 410 to determine the total mass of KCl absorbed by the VOG_mC_7 hydrogel. VOG_mC_7-KCl was then immersed in 200 mL of demineralized water, stirred slowly using a magnetic stirrer. Every ten minutes, 10 mL of the liquid used to immerse the VOG_mC_7-KCl hydrogel was pipetted, and in order to keep the volume of the system unchanged, immediately after pipetting, 10 mL of demineralized water was immediately added to the system. The quantity of KCl in the pipetted sample was then measured using a Corning 410 flame photometer instrument.

Acknowledgements

We are grateful to the Indonesian Government for the funding.

Conflict of Interest

The authors declare no conflict of interest.

Data Availability Statement

The data that support the findings of this study are available on request from the corresponding author. The data are not publicly available due to privacy or ethical restrictions.

Keywords: carbon nanotubes · controlled-release material · glutaraldehyde · poly(vinyl alcohol) · *Premna Oblongifolia* Merr

[1] S. Savci, *APCBEE Procedia* **2012**, *1*, 287–292.
[2] S. Savci, *Inter. J. Environ. Sci. Dev.* **2012**, *3*, 77–80.
[3] M. Udvardi, E. L. Brodie, W. Riley, S. Kaeppler, J. Lynch, *Procedia Environ. Sci.* **2015**, *29*, 303–303.
[4] K. Lubkowski, *Polish J. Chem. Techol.* **2016**, *18*, 72–79.
[5] R. Chandini, R. Kumar, O. Prakash, In: *Research Trends in Environmental Sciences* (Editor: P. Sharma), Chapter 5, 2nd Edition, AkiNik Publications, New Delhi, **2019**, 71–86.
[6] M. M. E. Costa, E. C. M. Cabral-Albuquerque, T. L. M. Alves, J. C. Pinto, R. L. Fialho, *J. Agric. Food Chem.* **2013**, *61*, 9984–9991.
[7] K. El-Rafaie, A. A. Sakran, *Ind. Eng. Chem. Res.* **1996**, *35*, 3726–3729.
[8] D. M. Andersen, P. M. Gilbert, J. M. Burkholder, *Estuaries* **2002**, *25*, 704–726..
[9] X-e. Yang, X. Wu, H-l. Hao, Z-l. He, *J. Zhejiang Univ. Sci. B* **2008**, *9*, 197–209.
[10] M. Karydis, *Global NEST Journal* **2009**, *11*, 373–390.
[11] A. Shaviv, *Ad. Agron.* **2001**, *71*, 1–49.
[12] M. E. Trenkel, *Slow- and Controlled-Release and Stabilized Fertilizers: An Option for Enhancing Nutrient Use Efficiency in Agriculture*, International Fertilizer Industry Association, Paris, France, **2010**, 14–15.
[13] M. Rajan, S. Shahena, V. Chandran, L. Mathew, In: *Controlled Release Fertilizers for Sustainable Agriculture* (Eds: F. B. Lawu, T. Volova, S. Thomas, K. R. Rakhimol), Chapter 3, Academic Press, London, **2021**, 41–56.
[14] X. Han, S. Chen, X. Hu, *Desalination* **2009**, *240*, 21–26.
[15] S. Fertahi, M. Ilsouk, Y. Zeroual, A. Oukarroum, A. Barakat, *J. Controlled Release* **2021**, *330*, 341–361.
[16] P. Vejan, T. Khadiran, R. Abdullah, N. Ahmad, *J. Control. Rel.* **2021**, *339*, 321–334.
[17] R. Liang, M. Liu, L. Wu, *React. Funct. Polym.* **2007**, *67*, 769–779.
[18] N. A. Peppas, A. R. Khare, *Adv. Drug Delivery Rev.* **1993**, *11*, 1–35.
[19] T. Jamnongkan, S. Kaewpirom, *J. Polym. Environ.* **2010**, *18*, 413–421.
[20] J. Maitra, V. K. Shukla, *Am. J. Polym. Sci.* **2014**, *4*, 25–31.
[21] M. F. Akhtar, M. Hanif, N. M. Ranjha, *Saudi Pharm. J.* **2016**, *24*, 554–559.
[22] E. Otsuka, S. Komiya, S. Sasaki, J. Xing, Y. Bando, Y. Hirashima, M. Sugiyama, A. Suzuki, *Soft Matter* **2012**, *8*, 8129–8136.
[23] H. Hendrawan, F. Khoerunnisa, F. I. Ekawati, Y. Sonjaya, *Mater. Phys. Mech.* **2019**, *42*, 141–150.
[24] E. F. Reisa, F. S. Campos, A. P. Lage, R. C. Leite, L. G. Heneine, W. L. Vasconcelos, Z. I. P. Lobato, H. S. Mansur, *Mater. Res.* **2006**, *9*, 185–191.
[25] H. Hosseinzadeh, *Curr. Chem. Lett.* **2013**, *2*, 153–158.
[26] W. E. Hennink, C. F. van Nostrum, *Adv. Drug Delivery Rev.* **2012**, *64*, 223–236.
[27] S. Noppakundilograt, N. Pheatcharat, S. Kiatkamjornwong, *J. Appl. Polym. Sci.* **2015**, *132*, 41249.
[28] H. Hendrawan, F. Khoerunnisa, Y. Sonjaya, A. D. Putri, *Iop. Conf. Ser. Mater. Sci. Eng.* **2019**, *509*, 012048.
[29] Z. Li, M. Tang, J. Dai, T. Wang, R. Bai, *Polymer* **2016**, *85*, 67–76.

[30] X. Tong, J. Zheng, Y. Lu, Z. Zhang, H. Cheng, *Mater. Lett.* **2007**, *61*, 1704–1706.
[31] N. S. Satarkar, D. Johnson, B. Marrs, R. Andrews, C. Poh, B. Gharaibeh, K. Saito, K. W. Anderson, J. Z. Hilt, *J. Appl. Polym. Sci.* **2010**, *117*, 1813–1819.
[32] S. D. Park, D. H. Han, D. Teng, Y. Kwon, *Curr. Appl. Phys.* **2008**, *8*, 482–485.
[33] M. Theodore, M. Hosur, J. Thomas, S. Jeelani, *Mater. Sci. Eng. A* **2011**, *528*, 1192–1200.
[34] T. A. Holland, J. K. V. Tessmar, Y. Tabata, A. G. Mikos, *J. Controlled Release* **2004**, *94*, 101–114.
[35] J. W. Lim, H-j. Kim, Y. Kim, S. G. Shin, S. Cho, S. W. G. Jung, J. H. Jeong, *Polymer* **2020**, *12*, 583.
[36] H. S. Mansur, C. M. Sadahira, A. N. Souza, A. A. P. Mansur, *Mater. Sci. Eng.* **2008**, *28*, 539–548.
[37] C. Yeom, K. Lee, *J. Membr. Sci.* **1996**, *109*, 257–285.
[38] J. M. Mishra, F. Ferreira, S. Kannan, *Carbohydr. Polym.* **2015**, *121*, 37–48.
[39] S. Vural, K. B. Dikovics, D. M. Kalyon, *Soft Matter* **2010**. *6*, 3870–3875.
[40] K.-A. Leslie, R. Doane-Solomon, S. Arora, S. J. Curley, C. Szczepanski, M. M. Driscoll, *Soft Matter* **2021**, *17*, 1513–1520.
[41] X. Wang, W. Hong, *Soft Matter* **2012**, *8*, 8171–8178.
[42] N. Hayarti, Undergraduate thesis, Universitas Pendidikan (Indonesia), **2016**, can be found under http://repository.upi.edu/id/eprint/26696.

Manuscript received: November 14, 2022
Revised manuscript received: January 18, 2023